and related disorders. We also acknowledge the support of the Biomedical Research Core of Tohoku University Graduate School of Medicine. This work was supported by the Funding Program for the Next Generation of World-Leading Researchers (NEXT Program) from the Ministry of Education, Culture, Sports, Science, and Technology of Japan (MEXT) to Y.A. (LS004), by Grants-in-Aids from MEXT, from the Japan Society for the Promotion of Science, and from the Ministry of Health, Labor, and Welfare to Y.M. and T.N. This work was supported in part by the National Cancer Center Research and Development Fund (23-22-11).

Received: April 23, 2013
Revised: May 19, 2013
Accepted: May 23, 2013
Published: June 20, 2013

Web Resources

The URLs for data presented herein are as follows:

Catalogue of Somatic Mutations in Cancer (COSMIC), http://www.sanger.ac.uk/genetics/CGP/cosmic/
Online Mendelian Inheritance in Man (OMIM), http://www.omim.org
RefSeq, http://www.ncbi.nlm.nih.gov/RefSeq
The RAS/MAPK Syndromes Homepage, http://www.medgen.med.tohoku.ac.jp/RasMapk%20syndromes.html

References

1. Takai, Y., Sasaki, T., and Matozaki, T. (2001). Small GTP-binding proteins. Physiol. Rev. *81*, 153–208.
2. Giehl, K. (2005). Oncogenic Ras in tumour progression and metastasis. Biol. Chem. *386*, 193–205.
3. Romano, A.A., Allanson, J.E., Dahlgren, J., Gelb, B.D., Hall, B., Pierpont, M.E., Roberts, A.E., Robinson, W., Takemoto, C.M., and Noonan, J.A. (2010). Noonan syndrome: clinical features, diagnosis, and management guidelines. Pediatrics *126*, 746–759.
4. van der Burgt, I. (2007). Noonan syndrome. Orphanet J. Rare Dis. *2*, 4.
5. Tartaglia, M., Mehler, E.L., Goldberg, R., Zampino, G., Brunner, H.G., Kremer, H., van der Burgt, I., Crosby, A.H., Ion, A., Jeffery, S., et al. (2001). Mutations in PTPN11, encoding the protein tyrosine phosphatase SHP-2, cause Noonan syndrome. Nat. Genet. *29*, 465–468.
6. Digilio, M.C., Conti, E., Sarkozy, A., Mingarelli, R., Dottorini, T., Marino, B., Pizzuti, A., and Dallapiccola, B. (2002). Grouping of multiple-lentigines/LEOPARD and Noonan syndromes on the PTPN11 gene. Am. J. Hum. Genet. *71*, 389–394.
7. Schubbert, S., Zenker, M., Rowe, S.L., Böll, S., Klein, C., Bollag, G., van der Burgt, I., Musante, L., Kalscheuer, V., Wehner, L.E., et al. (2006). Germline KRAS mutations cause Noonan syndrome. Nat. Genet. *38*, 331–336.
8. Roberts, A.E., Araki, T., Swanson, K.D., Montgomery, K.T., Schiripo, T.A., Joshi, V.A., Li, L., Yassin, Y., Tamburino, A.M., Neel, B.G., and Kucherlapati, R.S. (2007). Germline gain-of-function mutations in SOS1 cause Noonan syndrome. Nat. Genet. *39*, 70–74.
9. Tartaglia, M., Pennacchio, L.A., Zhao, C., Yadav, K.K., Fodale, V., Sarkozy, A., Pandit, B., Oishi, K., Martinelli, S., Schackwitz, W., et al. (2007). Gain-of-function SOS1 mutations cause a distinctive form of Noonan syndrome. Nat. Genet. *39*, 75–79.
10. Pandit, B., Sarkozy, A., Pennacchio, L.A., Carta, C., Oishi, K., Martinelli, S., Pogna, E.A., Schackwitz, W., Ustaszewska, A., Landstrom, A., et al. (2007). Gain-of-function RAF1 mutations cause Noonan and LEOPARD syndromes with hypertrophic cardiomyopathy. Nat. Genet. *39*, 1007–1012.
11. Razzaque, M.A., Nishizawa, T., Komoike, Y., Yagi, H., Furutani, M., Amo, R., Kamisago, M., Momma, K., Katayama, H., Nakagawa, M., et al. (2007). Germline gain-of-function mutations in RAF1 cause Noonan syndrome. Nat. Genet. *39*, 1013–1017.
12. Cirstea, I.C., Kutsche, K., Dvorsky, R., Gremer, L., Carta, C., Horn, D., Roberts, A.E., Lepri, F., Merbitz-Zahradnik, T., König, R., et al. (2010). A restricted spectrum of NRAS mutations causes Noonan syndrome. Nat. Genet. *42*, 27–29.
13. Cordeddu, V., Di Schiavi, E., Pennacchio, L.A., Ma'ayan, A., Sarkozy, A., Fodale, V., Cecchetti, S., Cardinale, A., Martin, J., Schackwitz, W., et al. (2009). Mutation of SHOC2 promotes aberrant protein N-myristoylation and causes Noonan-like syndrome with loose anagen hair. Nat. Genet. *41*, 1022–1026.
14. Loh, M.L., Sakai, D.S., Flotho, C., Kang, M., Fliegauf, M., Archambeault, S., Mullighan, C.G., Chen, L., Bergstraesser, E., Bueso-Ramos, C.E., et al. (2009). Mutations in CBL occur frequently in juvenile myelomonocytic leukemia. Blood *114*, 1859–1863.
15. Niemeyer, C.M., Kang, M.W., Shin, D.H., Furlan, I., Erlacher, M., Bunin, N.J., Bunda, S., Finklestein, J.Z., Sakamoto, K.M., Gorr, T.A., et al. (2010). Germline CBL mutations cause developmental abnormalities and predispose to juvenile myelomonocytic leukemia. Nat. Genet. *42*, 794–800.
16. Pérez, B., Mechinaud, F., Galambrun, C., Ben Romdhane, N., Isidor, B., Philip, N., Derain-Court, J., Cassinat, B., Lachenaud, J., Kaltenbach, S., et al. (2010). Germline mutations of the CBL gene define a new genetic syndrome with predisposition to juvenile myelomonocytic leukaemia. J. Med. Genet. *47*, 686–691.
17. Aoki, Y., Niihori, T., Kawame, H., Kurosawa, K., Ohashi, H., Tanaka, Y., Filocamo, M., Kato, K., Suzuki, Y., Kure, S., and Matsubara, Y. (2005). Germline mutations in HRAS proto-oncogene cause Costello syndrome. Nat. Genet. *37*, 1038–1040.
18. Niihori, T., Aoki, Y., Narumi, Y., Neri, G., Cavé, H., Verloes, A., Okamoto, N., Hennekam, R.C., Gillessen-Kaesbach, G., Wieczorek, D., et al. (2006). Germline KRAS and BRAF mutations in cardio-facio-cutaneous syndrome. Nat. Genet. *38*, 294–296.
19. Rodriguez-Viciana, P., Tetsu, O., Tidyman, W.E., Estep, A.L., Conger, B.A., Cruz, M.S., McCormick, F., and Rauen, K.A. (2006). Germline mutations in genes within the MAPK pathway cause cardio-facio-cutaneous syndrome. Science *311*, 1287–1290.
20. Aoki, Y., Niihori, T., Narumi, Y., Kure, S., and Matsubara, Y. (2008). The RAS/MAPK syndromes: novel roles of the RAS pathway in human genetic disorders. Hum. Mutat. *29*, 992–1006.
21. Tidyman, W.E., and Rauen, K.A. (2009). The RASopathies: developmental syndromes of Ras/MAPK pathway dysregulation. Curr. Opin. Genet. Dev. *19*, 230–236.
22. Groesser, L., Herschberger, E., Ruetten, A., Ruivenkamp, C., Lopriore, E., Zutt, M., Langmann, T., Singer, S., Klingseisen, L., Schneider-Brachert, W., et al. (2012). Postzygotic HRAS and KRAS mutations cause nevus sebaceous and Schimmelpenning syndrome. Nat. Genet. *44*, 783–787.

23. Abe, Y., Aoki, Y., Kuriyama, S., Kawame, H., Okamoto, N., Kurosawa, K., Ohashi, H., Mizuno, S., Ogata, T., Kure, S., et al.; Costello and CFC syndrome study group in Japan. (2012). Prevalence and clinical features of Costello syndrome and cardio-facio-cutaneous syndrome in Japan: findings from a nationwide epidemiological survey. Am. J. Med. Genet. A. *158A*, 1083–1094.
24. Kobayashi, T., Aoki, Y., Niihori, T., Cavé, H., Verloes, A., Okamoto, N., Kawame, H., Fujiwara, I., Takada, F., Ohata, T., et al. (2010). Molecular and clinical analysis of RAF1 in Noonan syndrome and related disorders: dephosphorylation of serine 259 as the essential mechanism for mutant activation. Hum. Mutat. *31*, 284–294.
25. Komatsuzaki, S., Aoki, Y., Niihori, T., Okamoto, N., Hennekam, R.C., Hopman, S., Ohashi, H., Mizuno, S., Watanabe, Y., Kamasaki, H., et al. (2010). Mutation analysis of the SHOC2 gene in Noonan-like syndrome and in hematologic malignancies. J. Hum. Genet. *55*, 801–809.
26. Narumi, Y., Aoki, Y., Niihori, T., Neri, G., Cavé, H., Verloes, A., Nava, C., Kavamura, M.I., Okamoto, N., Kurosawa, K., et al. (2007). Molecular and clinical characterization of cardio-facio-cutaneous (CFC) syndrome: overlapping clinical manifestations with Costello syndrome. Am. J. Med. Genet. A. *143A*, 799–807.
27. Narumi, Y., Aoki, Y., Niihori, T., Sakurai, M., Cavé, H., Verloes, A., Nishio, K., Ohashi, H., Kurosawa, K., Okamoto, N., et al. (2008). Clinical manifestations in patients with SOS1 mutations range from Noonan syndrome to CFC syndrome. J. Hum. Genet. *53*, 834–841.
28. Niihori, T., Aoki, Y., Okamoto, N., Kurosawa, K., Ohashi, H., Mizuno, S., Kawame, H., Inazawa, J., Ohura, T., Arai, H., et al. (2011). HRAS mutants identified in Costello syndrome patients can induce cellular senescence: possible implications for the pathogenesis of Costello syndrome. J. Hum. Genet. *56*, 707–715.
29. Saito, Y., Aoki, Y., Muramatsu, H., Makishima, H., Maciejewski, J.P., Imaizumi, M., Rikiishi, T., Sasahara, Y., Kure, S., Niihori, T., et al. (2012). Casitas B-cell lymphoma mutation in childhood T-cell acute lymphoblastic leukemia. Leuk. Res. *36*, 1009–1015.
30. Li, H., and Durbin, R. (2009). Fast and accurate short read alignment with Burrows-Wheeler transform. Bioinformatics *25*, 1754–1760.
31. McKenna, A., Hanna, M., Banks, E., Sivachenko, A., Cibulskis, K., Kernytsky, A., Garimella, K., Altshuler, D., Gabriel, S., Daly, M., and DePristo, M.A. (2010). The Genome Analysis Toolkit: a MapReduce framework for analyzing next-generation DNA sequencing data. Genome Res. *20*, 1297–1303.
32. Wang, K., Li, M., and Hakonarson, H. (2010). ANNOVAR: functional annotation of genetic variants from high-throughput sequencing data. Nucleic Acids Res. *38*, e164.
33. Lee, C.H., Della, N.G., Chew, C.E., and Zack, D.J. (1996). Rin, a neuron-specific and calmodulin-binding small G-protein, and Rit define a novel subfamily of ras proteins. J. Neurosci. *16*, 6784–6794.
34. Wes, P.D., Yu, M., and Montell, C. (1996). RIC, a calmodulin-binding Ras-like GTPase. EMBO J. *15*, 5839–5848.
35. van der Burgt, I., Kupsky, W., Stassou, S., Nadroo, A., Barroso, C., Diem, A., Kratz, C.P., Dvorsky, R., Ahmadian, M.R., and Zenker, M. (2007). Myopathy caused by HRAS germline mutations: implications for disturbed myogenic differentiation in the presence of constitutive HRas activation. J. Med. Genet. *44*, 459–462.
36. Niwa, H., Yamamura, K., and Miyazaki, J. (1991). Efficient selection for high-expression transfectants with a novel eukaryotic vector. Gene *108*, 193–199.
37. Rusyn, E.V., Reynolds, E.R., Shao, H., Grana, T.M., Chan, T.O., Andres, D.A., and Cox, A.D. (2000). Rit, a non-lipid-modified Ras-related protein, transforms NIH3T3 cells without activating the ERK, JNK, p38 MAPK or PI3K/Akt pathways. Oncogene *19*, 4685–4694.
38. Shi, G.X., and Andres, D.A. (2005). Rit contributes to nerve growth factor-induced neuronal differentiation via activation of B-Raf-extracellular signal-regulated kinase and p38 mitogen-activated protein kinase cascades. Mol. Cell. Biol. *25*, 830–846.
39. Cai, W., Rudolph, J.L., Harrison, S.M., Jin, L., Frantz, A.L., Harrison, D.A., and Andres, D.A. (2011). An evolutionarily conserved Rit GTPase-p38 MAPK signaling pathway mediates oxidative stress resistance. Mol. Biol. Cell *22*, 3231–3241.
40. Runtuwene, V., van Eekelen, M., Overvoorde, J., Rehmann, H., Yntema, H.G., Nillesen, W.M., van Haeringen, A., van der Burgt, I., Burgering, B., and den Hertog, J. (2011). Noonan syndrome gain-of-function mutations in NRAS cause zebrafish gastrulation defects. Dis Model Mech *4*, 393–399.
41. Fürthauer, M., Van Celst, J., Thisse, C., and Thisse, B. (2004). Fgf signalling controls the dorsoventral patterning of the zebrafish embryo. Development *131*, 2853–2864.
42. Burch, M., Sharland, M., Shinebourne, E., Smith, G., Patton, M., and McKenna, W. (1993). Cardiologic abnormalities in Noonan syndrome: phenotypic diagnosis and echocardiographic assessment of 118 patients. J. Am. Coll. Cardiol. *22*, 1189–1192.
43. Schubbert, S., Shannon, K., and Bollag, G. (2007). Hyperactive Ras in developmental disorders and cancer. Nat. Rev. Cancer *7*, 295–308.
44. Kratz, C.P., Rapisuwon, S., Reed, H., Hasle, H., and Rosenberg, P.S. (2011). Cancer in Noonan, Costello, cardiofaciocutaneous and LEOPARD syndromes. Am. J. Med. Genet. C. Semin. Med. Genet. *157*, 83–89.
45. Denayer, E., Devriendt, K., de Ravel, T., Van Buggenhout, G., Smeets, E., Francois, I., Sznajer, Y., Craen, M., Leventopoulos, G., Mutesa, L., et al. (2010). Tumor spectrum in children with Noonan syndrome and SOS1 or RAF1 mutations. Genes Chromosomes Cancer *49*, 242–252.
46. Jongmans, M.C.J., Hoogerbrugge, P.M., Hilkens, L., Flucke, U., van der Burgt, I., Noordam, K., Ruiterkamp-Versteeg, M., Yntema, H.G., Nillesen, W.M., Ligtenberg, M.J.L., et al. (2010). Noonan syndrome, the SOS1 gene and embryonal rhabdomyosarcoma. Genes Chromosomes Cancer *49*, 635–641.
47. Hynds, D.L., Spencer, M.L., Andres, D.A., and Snow, D.M. (2003). Rit promotes MEK-independent neurite branching in human neuroblastoma cells. J. Cell Sci. *116*, 1925–1935.
48. Anastasaki, C., Estep, A.L., Marais, R., Rauen, K.A., and Patton, E.E. (2009). Kinase-activating and kinase-impaired cardio-facio-cutaneous syndrome alleles have activity during zebrafish development and are sensitive to small molecule inhibitors. Hum. Mol. Genet. *18*, 2543–2554.

The European Journal of Orthodontics Advance Access published May 9, 2013

European Journal of Orthodontics
doi:10.1093/ejo/cjt019

Cervical characteristics of Noonan syndrome

Jun J. Miyamoto*, Tomoe Yabunaka* and Keiji Moriyama*,**
*Departments of Maxillofacial Orthognathics, Graduate School and **Global Center of Excellence Program for the International Research Center for Molecular Science in Tooth and Bone Disease, Tokyo Medical and Dental University, Tokyo, Japan

Correspondence to: Keiji Moriyama, Section of Maxillofacial Orthognathics, Graduate School, Tokyo Medical and Dental University, 1-5-45 Yushima, Bunkyo-ku, Tokyo 113-8549, Japan. E-mail: k-moriyama.mort@tmd.ac.jp

SUMMARY

BACKGROUND/OBJECTIVES A short neck and low posterior hairline are characteristics of Noonan syndrome (NS) and are hallmarks of basilar invagination/impression. However, it is seldom that NS has been directly linked with this symptom. Thus, this study aimed to investigate basilar impression in NS subjects compared with control subjects and individuals exhibiting Turner Syndrome (TS).

SUBJECTS/METHODS The degree of basilar impression and vertical positional differences of the third and fourth cervical vertebrae and hyoid bone in NS (n = 9, mean age: 12.1 years), TS (n = 9, mean age: 12.1 years), and control subjects (n = 9, mean age: 12.0 years) were investigated using lateral cephalometric radiographs. Differences between the three groups were compared using the Steel–Dwass test. Vertical positional differences in the anatomical structures within each group were compared using the Wilcoxon signed-rank test accompanied by a Bonferroni–Holm correction.

RESULTS The distance by which the odontoid tip extended past McGregor's line in subjects with NS was significantly greater compared with TS and control subjects. The third and fourth cervical vertebrae were positioned significantly superiorly in subjects with NS compared with TS and control subjects and, in NS, were also significantly superior to the hyoid bone. There was no difference in the position of the hyoid bone itself between the groups.

CONCLUSION/IMPLICATION These results suggest that basilar impression may be a frequently found symptom of NS.

Introduction

Noonan syndrome (NS; OMIM 163950) is an autosomal dominant condition in which approximately 50 per cent of cases are caused by missense mutations in the PTPN11 gene that encodes Shp-2, a regulatory component of the Ras-mitogen-activated protein kinase (Ras-MAPK) signalling network. In contrast, genetic anomalies in other Ras-MAPK pathway genes, such as KRAS, SOS1, and Raf-1, play only a minor role in the molecular pathogenesis of the disease (Ferrero *et al.*, 2008). NS is characterized clinically by a pattern of typical facial dysmorphism, malformations including congenital cardiac defects, short stature, abnormal chest shape, a broad or webbed neck, and a variable learning disability (Turner, 2011; van der Burgt, 2007). Other characteristics are a short neck and low posterior hairline (van der Burgt, 2007). Reduced neck length and low hairline have been recognized as hallmarks of basilar invagination for several decades, and reduced neck length is considered a diagnostic feature of basilar invagination (Goel and Shah, 2009). In a previous study, patients with basilar invagination underwent atlanto-axial joint distraction as a putative treatment modality, with clinical and radiological analysis of the resultant physical and morphological changes in the neck. These experiments suggested that an asymptomatic short neck could be indicative of basilar invagination (Goel and Shah, 2009).

Another reported characteristic feature of NS is malocclusion (Collins and Turner, 1973; Horowitz and Morishima, 1974; Shaw *et al.*, 2007). Thus, patients with NS often have need for orthodontic consultation. Several clinical reports describing such consultations have been published (Asokan *et al.*, 2007; Emral and Akcam, 2009; Ierardo *et al.*, 2010). Other orthodontic studies have reported abnormal radiographic findings in the cervical vertebrae, such as basilar invagination/impression (Vastardis and Evans, 1996; Soni *et al.*, 2008). Such findings during cephalometric analysis were made possible because radiological diagnosis of basilar invagination/impression can be established using constructed lines on the lateral cephalogram (Soni *et al.*, 2008).

It has been previously reported that the Arnold-Chiari malformation is also a characteristic of NS (Peiris and Ball, 1982; Gabrielli *et al.*, 1990; Holder-Espinasse and Winter, 2003; Galarza *et al.*, 2010), but there is only one case study directly linking NS with basilar invagination (Miyoshi *et al.*, 2011). Thus, it is unclear whether basilar invagination/impression is a characteristic of NS.

Turner Syndrome (TS) is a phenotypically similar disorder to NS and shares several NS characteristics, such as short stature, webbed neck, low posterior hairline, and partially similar facial features (Gardner *et al.*, 2007), although the presence of chromosomal defects in the

aetiology of TS distinguish it from NS (van Der Burgt and Brunner, 2000; Delgado-López *et al.*, 2007). Therefore, the aim of this study was to systematically investigate basilar invagination/impression in NS compared with control subjects (lacking any congenital anomalies) and individuals with TS.

Subjects and methods

Subjects

Twenty-seven Japanese subjects participated after giving fully informed consent as required by the protocol, which was approved by the institutional ethics committee (approval #419). Participants were classified into three groups ($n = 9$ in each group): the NS group comprised subjects with NS (five males, four females; mean age: 12.1±2.3 years), the TS group comprised subjects with TS, age-matched to the NS subjects (nine females; mean age: 12.1±2.4 years), and the control group comprised subjects with no congenital anomalies and were age- and gender-matched with subjects in the NS group (five males, four females; mean age: 12.0±2.2 years). Patients with NS and TS were diagnosed at hospitals containing a paediatric department. The karyotypes of TS subjects were unknown. All subjects were devoid of any missing erupted and successional permanent teeth (except for the third molars) and had no cleft lip and/or palate.

Cephalometric analysis

Lateral cephalometric radiographs were taken using a cephalostat (AXIOM Aristos MX/VX; Siemens, Tokyo, Japan). Patients were positioned with teeth in the intercuspal position and with a standing mirror-guided natural head position checked by dental radiologists, such that the degree of basilar impression and any vertical differences in the position of the third and fourth cervical vertebra and the hyoid bone could be simultaneously evaluated. In this study, we measured actual length. The magnification in the lateral cephalometric radiographs is 1.1 times and the results took into account the magnification.

The degree of basilar impression was measured as the distance by which the odontoid tip extended past McGregor's line, drawn from the posterior hard palate to the lowest point on the midline occipital curve (Figure 1). Basilar impression is defined as odontoid tip migration of 4.5 mm or more past McGregor's line (McGregor, 1948).

The vertical positions of the third and fourth cervical vertebra (C3 and C4, respectively) and the hyoid bone (H) were measured by extending a horizontal line from a reference point on each to intersect with a vertical (superior-inferior) line dropped from the sella turcica (S) (Figure 2). These reference points were derived from a previous report describing C3 and C4 references as being the most antero-inferior point of the body of these vertebrae, while the H reference was the most antero-superior point of the body of the hyoid bone (Kollias and Krogstad, 1999; Ricketts, 1989) (Figure 2).

To eliminate experimental errors, the same investigator traced all cephalometric radiographs, and the method error for each parameter was calculated by comparing duplicate tracings at an interval of at least 2 weeks. Errors for a single measurement of linear variables were calculated using the following formula (Dahlberg, 1940):

$$\text{Method error} = \left(\sum \frac{d^2}{2n}\right)^{\frac{1}{2}}$$

where d is the difference between measured pairs and n is the number of pairs.

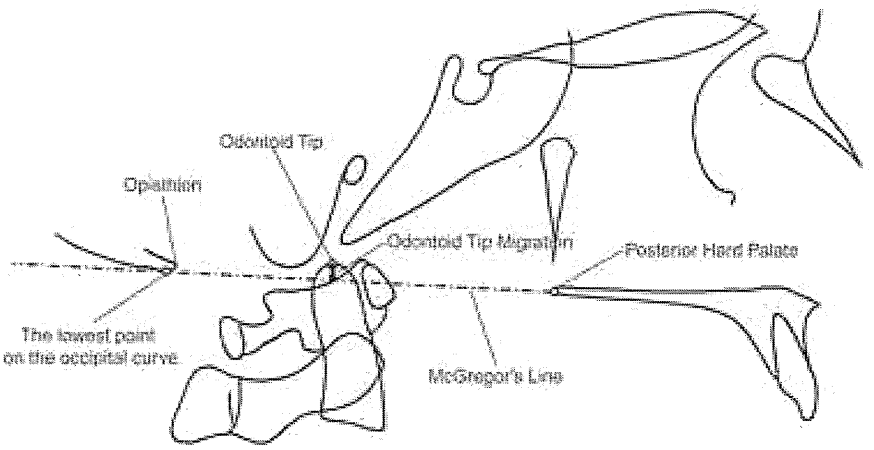

Figure 1 Illustration showing the odontoid tip and McGregor's line, which is used to assess superior odontoid migration. The dashed-dotted lines show McGregor's line, and the distance by which the odontoid tip extends past McGregor's line is indicated by an arrow.

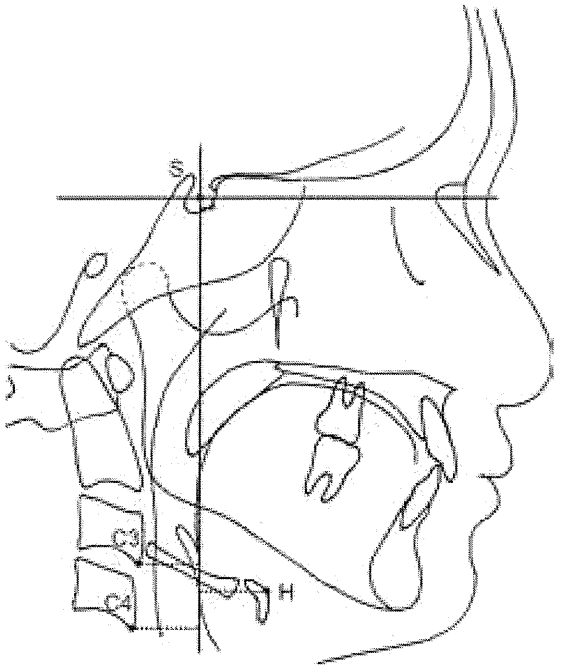

Figure 2 Cervicocraniofacial skeletal reference points used in this study. 'C3', 'C4', and 'H' denote the third cervical vertebra, fourth cervical vertebra, and hyoid bone, respectively. Solid lines show a horizontal line parallel to the floor and a vertical line perpendicular to this horizontal line passing through the sella turcica (S), against which the vertical position of C3, C4, and H can be measured.

Statistical analysis

Differences in linear measurements in the NS, TS, and control groups were examined using a Kruskal–Wallis test with *post hoc* Steel–Dwass analysis, a non-parametric multiple comparison procedure. Differences within each group with regard to the vertical positions of C3, C4, and H were statistically evaluated using the Friedman test and *post hoc* analysis using the Wilcoxon signed-rank test accompanied by a Bonferroni–Holm correction, a non-parametric statistical hypothesis test used when comparing two related or matched samples. A threshold of $P < 0.05$ was considered statistically significant for the Kruskal–Wallis, Steel–Dwass, and Friedman tests, and adjusted P-values were compared with 0.05 using a Wilcoxon signed-rank test with a Bonferroni–Holm correction (Chan *et al.*, 2007).

Results

Representative lateral cephalometric radiographs from the NS, TS, and control groups are shown in Figure 3, with McGregor's line and anatomical structures indicated on each. In the NS group, the odontoid tip, C3, and C4 were all located superiorly to their respective positions in the TS and control groups.

Clinical features of the subjects

Three NS subjects had a short neck and six had a low posterior hairline. In contrast no TS subjects had a short neck, but three TS subjects had a low posterior hairline. Two NS subjects had both symptoms.

Method error

Overall, the mean and standard deviation of the method error was 0.35 ± 0.09 mm for linear measurements. When compared with previous studies (Hiyama *et al.*, 2001), no systematic errors were found.

Degree of basilar impression

Basilar impression is defined as extension of the odontoid tip 4.5 mm or more past McGregor's line (McGregor, 1948). This was the case for seven subjects in the NS group, one subject in the TS group, and no subjects in the control

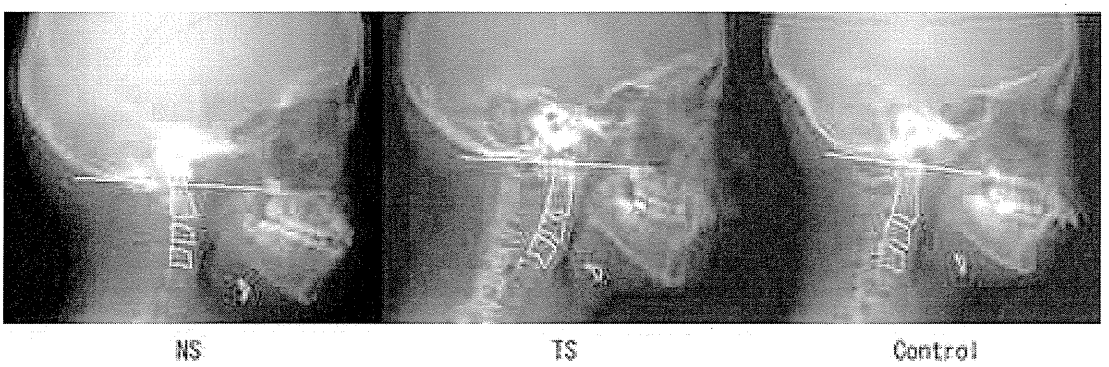

Figure 3 Representative lateral cephalometric radiographs of subjects in the NS, TS, and control groups. White lines denote McGregor's line for each subject. NS, Noonan syndrome; TS, Turner syndrome.

group. The median distance by which the odontoid tip extended past McGregor's line in the NS, TS, and control groups was 7.0, 3.0, and 1.5 mm, respectively (Figure 4A). Statistical analysis using the Kruskal–Wallis test and Steel–Dwass *post hoc* test revealed significant differences between the groups, specifically between the NS and TS or NS and control groups. However, there was no significant difference between the TS and control groups. Between-group comparisons, adjusted for multiple testing by the Steel–Dwass test, are shown in Figure 4B.

Vertical position of the third and fourth cervical vertebrae and the hyoid bone

The Kruskal–Wallis test revealed significant differences between the groups with regard to the vertical position of C3 and C4 but not H. Steel–Dwass comparison showed that the vertical position of C3 was significantly more superior in the NS group compared with the TS and control groups. The same analysis demonstrated no significant difference between the TS and control groups. A similar comparison of the vertical position of C4 revealed it to be significantly more superior in the NS group compared with the TS and control groups. The same analysis demonstrated no significant difference between the TS and control groups. There were no significant differences between the groups with regard to the vertical position of the hyoid bone (H) (Figure 5).

The Freidman test revealed significant differences within each group with regard to the vertical anatomical positions of C3, C4, and the hyoid bone. Comparison of the vertical positions using the Wilcoxon signed-rank test accompanied by a Bonferroni–Holm correction revealed that, in all groups, C3 was located significantly superior to C4. In the NS group, C3 and C4 were located significantly superior to the hyoid bone (Figure 5). In the TS group, C3, but not C4, was located significantly superior to the hyoid bone, whereas in the control group, C3 and C4 were significantly superior and inferior, respectively, in relation to the hyoid bone (Figure 5).

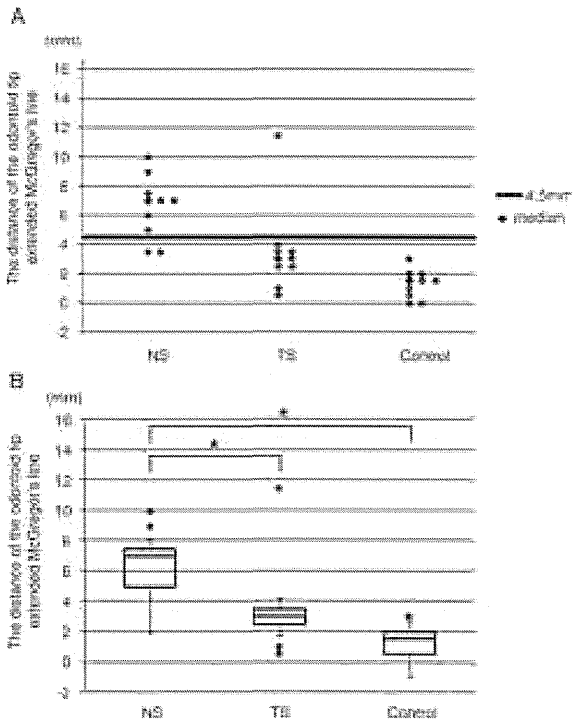

Figure 4 Distance by which the odontoid tip extends past McGregor's line in the NS, TS, and control groups. A, Individual data from all subjects. The horizontal line represents the criterion value of basilar invagination (4.5 mm). B, Data from A are represented as the median value enclosed by the 25th and 75th percentiles (box). Error bars represent 1.5 times the interquartile range of the lower and upper quartile. Data not included between the error bars are plotted as outliers (closed circle). *denotes a significant difference between the groups indicated ($P < 0.05$). NS, Noonan syndrome; TS, Turner syndrome.

Discussion

The present study describes cephalometric analysis aimed at evaluating the position of the cervical vertebrae in NS, TS, and control subjects.

The terms 'basilar impression' and 'basilar invagination' have been used synonymously. Kovero and colleagues defined basilar invagination as a protrusion of the odontoid process into the foramen magnum. This anomaly is apparent from the relation of the dens point to the foramen magnum line (McRae line). The area of the odontoid process that lies above one or several of the reference lines (Chamberlain line, McGregor line, or the baseline for the perpendicular distance from the tip of the odontoid process to a line parallel to the nasion-sella line and drawn through the lowermost point of the posterior cranial base) indicates basilar impression (Kovero *et al.*, 2006). Thus, the term relevant to our results is specified as 'basilar impression', those used in a general sense are specified as 'basilar invagination/impression'.

In the present study, there were three TS subjects with a low posterior hairline, but without basilar impression. Conversely, there were six NS subjects with a low posterior hairline and three with a short neck. Among them, two subjects had both symptoms. One subject with both symptoms and four subjects with a low posterior hairline had basilar impression. In this study, NS subjects with a low posterior hairline were associated with a high probability of basilar impression.

There are currently no reports describing basilar invagination/impression in TS patients. A previous study of basilar invagination/impression in osteogenesis imperfecta (OI) compared 54 OI patients with 108 healthy subjects (Kovero *et al.*, 2006) and found a mean distance of odontoid tip extension past McGregor's line of 2.3 mm in healthy subjects. In the present study, we calculated an equivalent

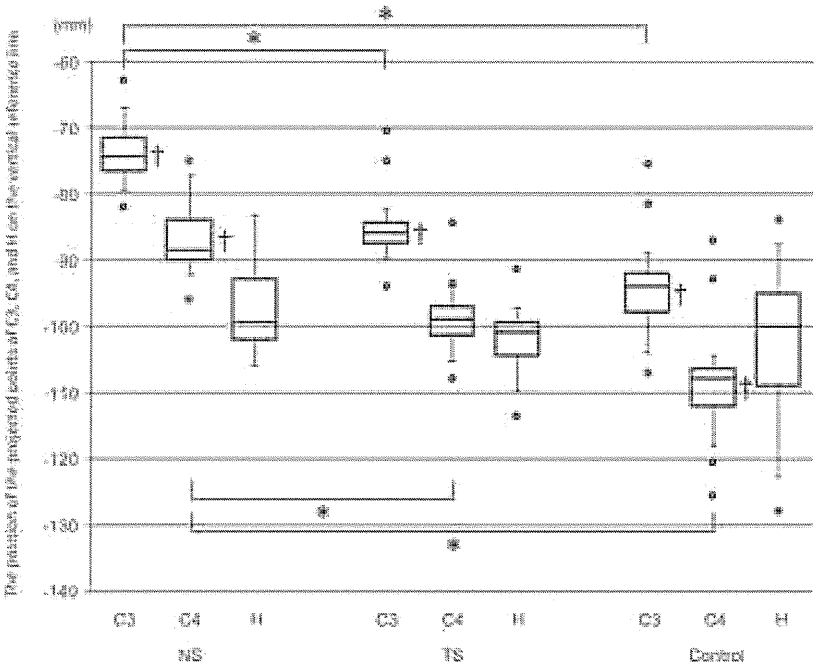

Figure 5 Positions of C3, C4, and H relative to the vertical reference line in the NS, TS, and control groups. The origin of the coordinate axes is the sella turcica and the more inferior the position of the projected point relative to this origin, the smaller the value assigned to it. Data are represented as the median value enclosed by the 25th and 75th percentiles (box). Error bars represent 1.5 times the interquartile range of the lower and upper quartile. Data not included between the error bars are plotted as outliers (closed circle). Asterisk denotes a significant difference between the indicated groups ($P < 0.05$). Dagger symbol denotes a significant difference in the vertical positions between C3 or C4 and the hyoid bone within each group. There were significant differences between C3 and C4 among all groups, but these are omitted from the figure. NS, Noonan syndrome; TS, Turner syndrome; C3, third cervical vertebra; C4, fourth cervical vertebra; H, hyoid bone.

median distance of 1.5 mm in the control group, in reasonable agreement with this previous study, suggesting that our results are comparable to published data.

There is currently only a single report directly linking basilar invagination with NS (Miyoshi *et al.*, 2011). In the present study, the odontoid tip in seven out of nine subjects in the NS group extended 4.5 mm or more past McGregor's line, and the distance by which the odontoid tip extended past McGregor's line in this group was significantly greater compared with the TS and control groups. There are studies that have evaluated basilar invagination/impression using McGregor's line as a reference line. Basilar invagination/impression has been variably defined as the tip of the odontoid process located more than 4.5 (McGregor, 1948), 5 (Soni *et al.*, 2008), and 7 mm (Sillence, 1994) beyond McGregor's line. In the present study, there were seven out of nine subjects (77.8 per cent) with odontoid tip migration of 4.5 mm or more in the NS group, six out of nine subjects (66.7 per cent) with migration more than 5 mm (except one subject with exactly 5 mm), and three out of nine subjects (33.3 per cent) with migration more than 7 mm (except two subjects with exactly 7 mm). In a previous study, it was stated that the odontoid apex should not lie above the criterion distance from McGregor's line in 90 per cent of individuals (Yochum and Lindsay, 2005). In other words, only 10 per cent of subjects would have the odontoid apex below it in the general population. In this study, the percentages of NS subjects with the odontoid apex above it were higher with regard to any of the criteria above.

Basilar invagination/impression is indicative of a cephalad position of the upper cervical vertebra relative to the base of the skull (Guebert *et al.*, 2005). Common signs and symptoms include muscle weakness, neck pain, posterior column dysfunction, bowel and bladder disturbance, and paraesthesia (Goel *et al.*, 1998). However, a large proportion of deformities of the craniovertebral junction, particularly skeletal anomalies, are asymptomatic. Indeed, symptoms were absent in 60 per cent (of 52 cases) of radiologically demonstrable cases of basilar impression (Burrows, 1981), and in 100 per cent of the NS subjects in the present study. The lack of literature reporting coincident NS and basilar invagination/impression may stem from the fact that most NS patients with basilar invagination/impression, being asymptomatic, fail to consult a neurologist.

We found that the positions of C3 and C4, but not the hyoid bone, in the NS group were significantly superior to those in the TS and control groups, suggesting that

basilar impression might be a frequently found symptom of NS. Although the relationship between the positions of the cervical vertebrae and the hyoid bone has not been reported in TS, it has been investigated in healthy subjects (Moore and Dalley, 1999; Standring, 2008). We found that in the control group using the horizontal line, C3 was significantly superior to the hyoid bone, whereas C4 was significantly inferior to the hyoid bone. In a previous study using CT images and the FH plane as a reference, the centre of the body of the hyoid bone was most often at the level of C4, despite the hyoid bone being consistently described in contemporary anatomy textbooks as being level with C3 (Mirjalili *et al.*, 2012). The authors postulated that this disparity might relate to the use, by anatomy textbooks, of both the body and greater horn of the hyoid bone to describe its vertebral level, whereas they measured only from the centre of the body of the hyoid bone. The authors also pointed out that the vertebral level of the body of the hyoid bone seen in tracings of the lateral cervical radiograph varies depending on which reference plane is used (Figure 6). We measured the orientation of a horizontal reference line and FH plane in the control group according to Madsen's method (Madsen *et al.*, 2008) and confirmed that the average orientation was -3.28 ± 4.01 degrees similar to that reported in Madsen *et al* (-4.82 ± 4.63 degrees in that study). In agreement with the Mirjalili study, there was no difference in the statistical results when the FH plane was used instead (data not shown) or in the centres of both the hyoid bone and C4 as references, the reference point H in eight control subjects was located approximately level with the fourth cervical vertebra (data not shown). However, because in the present study we used alternative reference points for C3 and C4 (i.e. their most antero-inferior points) and the hyoid bone (i.e. its most antero-superior point) (Figure 6), the reference point of H was located significantly superior to the reference point in C4, despite the anatomy being demonstrably normal and in agreement with previous studies. We believe that this accounts for any discrepancy between our data and previous studies.

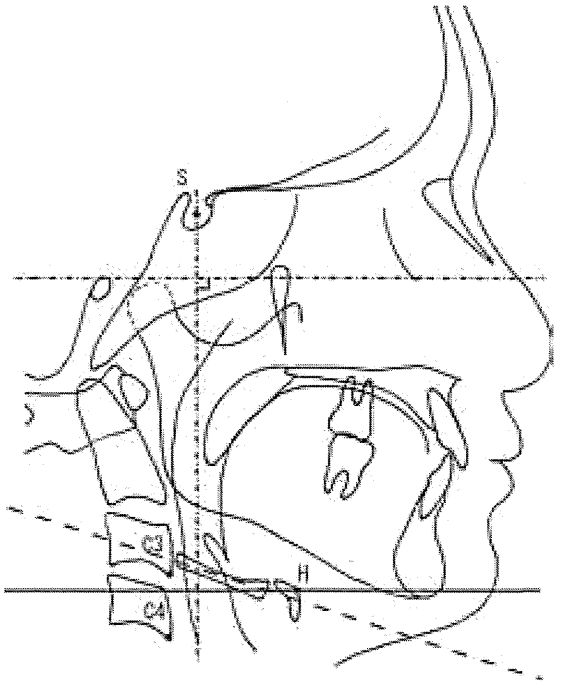

Figure 6 The vertebral level of structures in the neck depends in part on the choice of the reference plane. The solid line parallel to the Frankfort horizontal (FH) plane is not identical to the dashed line based on the inclination of the hyoid bone. The dashed-dotted lines show the FH plane and the reference line perpendicular to this originating in the sella turcica. Abbreviations: S, Sella; C3, the most antero-inferior point of the third cervical vertebra; C4, the most antero-inferior point of the fourth cervical vertebra; H, the most antero-superior point of the hyoid bone.

In this study, the number of subjects was small. However, it is difficult to recruit sufficient numbers of NS and TS subjects because they are rare syndromes. Further studies should investigate the results found here in a larger number of NS subjects. However, most previous studies listing cervical spine malformations commonly found in a variety of syndromes (Vastardis and Evans, 1996; Soni *et al.*, 2008) did not include NS in their analysis, depriving clinicians of an easy reference for recognizing and diagnosing NS in relation to other conditions affecting the cervical vertebrae. Our findings may help orthodontists recognize NS through the detection of basilar impression, a frequently found symptom of this syndrome, using cephalograms when patients attend orthodontic clinics for correction of malocclusion.

Conclusion

In the current study, we found that the odontoid tip extended significantly further past McGregor's line in the NS group compared with the TS and control groups, and that the positions of the third and the fourth cervical vertebrae in the NS group were significantly superior to those in the TS and control groups. Together, these data support a conclusion that basilar impression may be found frequently as a characteristic feature of NS.

Funding

Grants-in-Aid for Scientific Research Projects from the Japan Society for the Promotion of Science (#23792419); 'International Research Center for Molecular Science in Tooth and Bone Diseases', part of the Japanese Ministry of Education, Global Center of Excellence Program.

Acknowledgements

The authors would like to thank Assistant Professor Michiko Tsuji (Department of Maxillofacial Orthognathics,

Graduate School, Tokyo Medical and Dental University) for technical advice. We are indebted to Dr Keichi Kataoka, Dr Tomoko Ueno, and Dr Issareeya Ekprachayakoon for their help with data analysis, and we also gratefully acknowledge all other members of the Department of Maxillofacial Orthognathics, Graduate School, Tokyo Medical and Dental University for their support.

References

Asokan S, Muthu M S, Rathna Prabhu V 2007 Noonan syndrome: a case report. Journal of the Indian Society of Pedodontics and Preventive Dentistry 25: 144–147

Burrows E H 1981 Clinical relevance of radiological abnormalities of the craniovertebral junction. The British Journal of Radiology 54: 195–202

Chan A O *et al.* 2007 Prevalence of colorectal neoplasm among patients with newly diagnosed coronary artery disease.Journal of the American Medical Association 298: 1412–1419

Collins E, Turner G 1973 The Noonan syndrome–a review of the clinical and genetic features of 27 cases. The Journal of Pediatrics 83: 941–950

Dahlberg G 1940 Statistical Methods for Medical and Biological Students. George Allen & Unwin Ltd, London.

Delgado-López P D, Martín-Velasco V, Galacho-Harriero A M, Castilla-Díez J M, Rodríguez-Salazar A, Echevarría-Iturbe C 2007 Large chondroma of the dural convexity in a patient with Noonan's syndrome. Case report and review of the literature. Neurocirugía (Asturias, Spain) 18: 241–246

Emral M E, Akcam M O 2009 Noonan syndrome: a case report. Journal of Oral Science 51: 301–306

Ferrero G B *et al.* 2008 Clinical and molecular characterization of 40 patients with Noonan syndrome. European Journal of Medical Genetics 51: 566–572

Gabrielli O *et al.* 1990 Magnetic resonance imaging in the malformative syndromes with mental retardation. Pediatric Radiology 21: 16–19

Galarza M, Martínez-Lage J F, Ham S, Sood S 2010 Cerebral anomalies and Chiari type 1 malformation. Pediatric Neurosurgery 46: 442–449

Gardner D G, Shoback D M, Greenspan F S 2007 Greenspan's Basic & Clinical Endocrinology. 8th edition. McGraw Hill Medical, New York.

Goel A, Bhatjiwale M, Desai K 1998 Basilar invagination: a study based on 190 surgically treated patients. Journal of Neurosurgery 88: 962–968

Goel A, Shah A 2009 Reversal of longstanding musculoskeletal changes in basilar invagination after surgical decompression and stabilization. Journal of Neurosurgery Spine 10: 220–227

Guebert G M, Rowe L J, Yochum T R, Thompson J R, Masia C J 2005 Congenital anomalies and normal skeletal variants. In: Yochum T R, Rowe L J (eds.). Essentials of Skeletal Radiology. 3rd ed. Lippincott Williams & Wilkins, Philadelphia, pp. 257–403.

Hiyama S, Ono T, Ishiwata Y, Kuroda T 2001 Changes in mandibular position and upper airway dimension by wearing cervical headgear during sleep. American Journal of Orthodontics and Dentofacial Orthopedics 120: 160–168

Holder-Espinasse M, Winter R M 2003 Type 1 Arnold-Chiari malformation and Noonan syndrome. A new diagnostic feature? Clinical Dysmorphology 12: 275

Horowitz S L, Morishima A 1974 Palatal abnormalities in the syndrome of gonadal dysgenesis and its variants and in Noonan's syndrome. Oral Surgery, Oral Medicine, and Oral Pathology 38: 839–844

Ierardo G, Luzzi V, Panetta F, Sfasciotti G L, Polimeni A 2010 Noonan syndrome: A case report. European Journal of Paediatric Dentistry 11: 97–100

Kollias I, Krogstad O 1999 Adult craniocervical and pharyngeal changes–a longitudinal cephalometric study between 22 and 42 years of age. Part I: Morphological craniocervical and hyoid bone changes. European Journal of Orthodontics 21: 333–344

Kovero O, Pynnönen S, Kuurila-Svahn K, Kaitila I, Waltimo-Sirén J 2006 Skull base abnormalities in osteogenesis imperfecta: a cephalometric evaluation of 54 patients and 108 control volunteers. Journal of Neurosurgery 105: 361–370

Madsen D P, Sampson W J, Townsend G C 2008 Craniofacial reference plane variation and natural head position. European Journal of Orthodontics 30: 532–540

McGregor M 1948 The significance of certain measurements of the skull in the diagnosis of basilar impression. British Journal of Radiology 21: 171–181

Mirjalili S A, McFadden S L, Buckenham T, Stringer M D 2012 Vertebral levels of key landmarks in the neck. Clinical Anatomy 25: 851–857

Miyoshi Y, Yasuhara T, Date I 2011 Noonan syndrome with occipito-atlantal dislocation and upper cervical cord compression due to C1 dysplasia and basilar invagination. Neurologia Medico-chirurgica 51: 463–466

Moore K L, Dalley A F 1999 Clinically Oriented Anatomy, 4th Edition. Lippincott Williams & Wilkins, Philadelphia.

Peiris A, Ball M J 1982 Chiari (type 1) malformation and syringomyelia in a patient with Noonan's syndrome. Journal of Neurology, Neurosurgery, and Psychiatry 45: 753–754

Ricketts R M 1989 Provocations and Perceptions in Cranio-facial Orthopedics - Dental Science and Facial Art. Rocky Mountain Inc., Denver, pp. 797–803

Shaw A C, Kalidas K, Crosby A H, Jeffery S, Patton M A 2007 The natural history of Noonan syndrome: a long-term follow-up study. Archives of Disease in Childhood 92: 128–132

Sillence D O 1994 Craniocervical abnormalities in osteogenesis imperfecta: genetic and molecular correlation. Pediatric Radiology 24: 427–430

Soni P, Sharma V, Sengupta J 2008 Cervical vertebrae anomalies-incidental findings on lateral cephalograms. The Angle Orthodontist 78: 176–180

Standring S 2008 Gray's Anatomy: The Anatomical Basis of Clinical Practice, 40th edition. Edinburgh, Churchill Livingstone, pp. 405

Turner A M 2011 Noonan syndrome. Journal of Paediatrics and Child Health. Published online 19 July 2011, doi: 10.1111/j.1440-1754.2010.01970.x

van der Burgt I 2007 Noonan syndrome. Orphanet Journal of Rare Diseases 2: 4

van Der Burgt I, Brunner H 2000 Genetic heterogeneity in Noonan syndrome: evidence for an autosomal recessive form. American Journal of Medical Genetics 94: 46–51

Vastardis H, Evans C A 1996 Evaluation of cervical spine abnormalities on cephalometric radiographs. American Journal of Orthodontics and Dentofacial Orthopedics 109: 581–588

Yochum T R, Lindsay R 2005 Measurements in skeletal radiology. In: Yochum T R, Rowe L J (eds.) Essentials of Skeletal Radiology. 3rd edn. Lippincott Williams & Wilkins, Philadelphia, pp.197–256

CASE REPORT

Surgical Treatment for Scoliosis in Patients With Shprintzen-Goldberg Syndrome

Kota Watanabe, MD,† Eijiro Okada, MD,† Kenjiro Kosaki, MD,‡ Takashi Tsuji, MD,† Ken Ishii, MD,† Masaya Nakamura, MD,† Kazuhiro Chiba, MD,† Yoshiaki Toyama, MD,† and Morio Matsumoto, MD†*

Background: Shprintzen-Goldberg syndrome (SGS) is characterized by craniosynostosis and marfanoid habitus. The clinical findings of SGS include neurological, cardiovascular, connective tissue, and skeletal abnormalities. Among these skeletal findings, developmental scoliosis is recognized in half of all patients with SGS. However, no earlier reports have described the surgical treatment of scoliosis associated with SGS.

Methods: Four patients (2 boys and 2 girls; mean age at the time of surgery, 7.3 ± 4.4 y) with SGS who underwent surgical treatment for progressive scoliosis were reviewed. The radiologic findings, operative findings, and perioperative complications were evaluated.

Results: The mean preoperative Cobb angle was 102.8 ± 16.9 degrees. The curve patterns were a double curve in 2 cases and a triple curve in 2 cases. Local kyphosis at the thoracolumbar area was recognized in all the cases with a mean kyphosis angle of 49 ± 16 degrees. Growing rod procedures were performed in 2 patients, and posterior correction and fusion were performed in 2 patients. The mean correction rate was 45% in the patients who underwent the growing rod procedures at the time of growing rod placement and 51% in the patients who underwent posterior correction and fusion. Dislodgement of the proximal anchors occurred in 3 of the 4 patients. One patient developed pseudoarthrosis. Two patients developed deep wound infections, and implant removal was necessary in 1 patient.

Conclusions: Surgical treatment for scoliosis in patients with SGS was associated with a high incidence of perioperative and postoperative complications including implant dislodgements and deep wound infections attributable to poor bone quality and a thin body habitus, which are characteristic clinical features of this syndrome. Careful preoperative surgical planning and postoperative care are critical for the surgical treatment of scoliosis associated with SGS, especially in infants requiring multiple surgeries.

From the Departments of *Advanced Therapy for Spine and Spinal Cord Disorders; †Orthopedic Surgery; and ‡Pediatrics, Keio University School of Medicine, Tokyo, Japan.

Supported by none.

No funding was received for this study from any of the following organizations: National Institutes of Health (NIH); Wellcome Trust; Howard Hughes Medical Institute (HHMI).

Reprints: Morio Matsumoto, MD, Department of Orthopedic Surgery, Keio University School of Medicine, 35 Shinanomachi, Shinjuku, Tokyo, #160-8582, Japan. E-mail: morio@sc.itc.keio.ac.jp.

Level of Evidence: Level IV.

Key Words: Shprintzen-Goldberg syndrome, scoliosis, surgical treatment

(*J Pediatr Orthop* 2011;31:186–193)

Shprintzen-Goldberg syndrome (SGS), which is characterized by craniosynostosis and marfanoid habitus, was first reported by Shprintzen and Goldberg[1] in 1982. To date, approximately 40 cases of SGS have been reported.[2–5] An abnormality in the *FBN1* gene, which is related to Marfan syndrome,[6] is regarded as 1 of susceptible genes for SGS,[7–9] although this remains to be clarified in further genetic studies.[7,10,11] The clinical features of SGS include neurological, cardiovascular, connective tissue, and skeletal abnormalities. The skeletal features of SGS, such as a tall stature, arachnodactyly, foot deformity, joint hypermobility, and developmental scoliosis are similar to those of Marfan syndrome. The characteristic features that distinguish SGS from Marfan syndrome are craniofacial anomalies such as hypertelorism, downward-slanting palpebral fissures, a high-arched palate, micrognathia, low-set and posteriorly rotated ears, dolichocephaly, and a high prominent forehead caused by craniosynostosis.[2–5] Among these skeletal findings, developmental scoliosis is recognized in 50% of all patients reported with SGS.[4] However, to the authors' knowledge, the surgical treatment of scoliosis in patients with SGS has not been reported to date. In this study, we report 4 patients with SGS who underwent surgical treatments for progressive scoliosis.

METHODS

Four patients (2 male and 2 female; mean age at time of surgery, 7.3 ± 4.4 y) who underwent surgical treatments for severe scoliosis were included in this study. The diagnoses of SGS were made by a pediatrician specializing in genetic diseases based on the combinations of specific, earlier reported clinical features.[2,3,5] In 1 of the 4 patients (patient 2), a missense mutation in the *FBN1* gene was identified using a polymerase chain reaction analysis. The patients were followed for 4.4 ± 1.5 years (range, 2.5 to 6 y) after their first surgeries. The medical charts and radiographs of all the patients were reviewed

retrospectively, and the preoperative treatment, preoperative clinical findings, radiographic findings, surgical treatment, and perioperative and postoperative complications were investigated.

RESULTS

The clinical findings, radiologic findings, clinical courses, and surgical outcomes of the patients are summarized in Tables 1, 2, and 3. In 3 of the 4 patients, trunk deformities were recognized soon after the child began to sit or stand (patients 1, 2, and 3). However, one patient (patient 2) did not visit a pediatrician until the age of 4 years, and another patient (patient 1) was not referred to an orthopaedic surgeon until the age of 3 years, at which time the deformity had deteriorated to an extremely severe condition. The parents of patient 3 refused any treatment for scoliosis, although the patient was seen by a plastic surgeon until the age of years. Thus, none of the patients received brace treatment before surgery, and the Cobb angles at the time of the first recognition of the deformities could not be evaluated. In the radiographic evaluations, a double major curve pattern and a triple major curve pattern were recognized in 2 patients each

TABLE 1. Clinical Findings of 4 Cases

	Case 1	Case 2	Case 3	Case 4
Sex	Female	Male	Female	Male
Weight at operation	12.4 kg	11.5 kg	33 kg	44 kg
Centile	− 1.4 SD	− 1.1 SD	− 0.1 SD	0.1 SD
Hight at operation	103 cm	98 cm	146 cm	164 cm
Centile	1.6 SD	1.5 SD	1.6 SD	1.9 SD
Craniofacial				
Dolichocephaly	+	+	+	+
Fine/sparse hair			+	
High/prominent forehead	+	+	+	+
Ocular proptosis	+	+	+	+
Hypertelorism	+	+	+	+
Downslanting palpebral fissures	+	+	+	+
Strabismus	+			+
High, narrow palatal arch		+		+
Dental malocclusion	+	+	+	+
Micrognathia		+	+	
Skeletal				
Arachnodactyly	+	+	+	+
Camptodactyly	+	+	+	
Foot deformity	+		+	+
Pectus carinatum			+	
Joint hypermobility	+	+	+	
Craniosynostosis	+	+	+	+
Scoliosis	+	+	+	+
Cardiovascular				
Aortic root dilation		+		+
Mireal prolapse		+		
Mitral regurgitation				+
Arterial septal defect	+			
Tricuspid regurgitation		+		
Neurological				
Mental retardation		+	+	+
Other				
Minimal subcutaneous fat	+	+	+	+
Skin hyperelasticity	+	+	+	+
Myopia ± astigmatism	+		+	

SD indicates standard deviation.

TABLE 2. Radiological Findings of 4 Cases

Case	Sex	Age at Recognition of Scoliosis	Age at Surgery*	Postoperative Observation	Curve Pattern	Sagittal Alignment	Cobb Angle of Major Curve (°)	Flexibility of Major Curves (%)*	Dural Ectasia†
1	F	6 mo	3 y 7 mo	4 y	Triple	Thoracolumbar kyphosis (57 degrees)	53 (T1-7) 103 (T7-L1)	Not known	+
2	M	10 mo	4 y 10 mo	5 y	Double	Thoracolumbar kyphosis (66 degrees)	79 (T4-11) 100 (T11-L4)	72 (T4-11) 50 (T11-L4)	+
3	F	10 mo	10 y	2 y	Double	Thoracolumbar kyphosis (44 degrees)	113 (T5-T11) 105 (T11-L4)	40 (T5-T11) 33 (T11-L4)	—
4	M	7 y	12 y	3 y	Triple	Thoracolumbar kyphosis (29 degrees)	64 (T1-7) 78 (T7-L1) 52 (L1-5)	25 (T1-7) 38 (T7-L1) 27 (L1-5)	+

*Measured on supine side-bending films.
†Evaluated on MRI images.
F indicates female; M, male; MRI, magnetic resonance imaging.

TABLE 3. Surgical Results of 4 Cases

Case	Sex	Age at Surgery*	Operative Method	Operative Time (Min)*	Estimated Blood Loss (g)*	Correction Rate of Main Thoracic Curve (%)†	Complication	Present Treatment
1	F	3 y 7 mo	Growing rod	235	80	67	Implant failure at cranial anchors after first rod elongation Fourth replacements of distal anchors performed Deep wound infection that was successfully treated Proximal junctional kyphosis of 74 degrees	Growing rod
2	M	4 y 10 mo	Growing rod	325	168	55	Intraoperative left facet hook dislodgement at T5 Deep wound infection after first rod elongation Distal anchor removal because of persistent infection Distal implants removal after revision of distal anchors because of recurrence of infection	Brace
3	F	10 y	Posterior correction and fusion	300	660	59	Reduction of motor evoked potentials during the curve correction Pseudarthrosis at distal end (L3/4), which was treated by posterior intervertebral fusion at L3/4 and L4/5	Brace
4	M	12 y	Posterior correction and fusion	298	1080	89	Intraoperative bilateral T1 transverse processes hook dislodgements with fracture Reduction of motor evoked potentials during the curve correction Revision surgery of replacing dislodged hooks with pedicle screws at cranial ends 6 mo after initial surgery Respiratory insufficiency that required reintubation for 3 d Distal junctional kyphosis of 13degrees at L4/5	No

*Initial surgery for growing rod placement in case 1 and 2.
†Correction rates were calculated as a percentage change from the preoperative measurements.
F indicates female; M, male.

(Table 2). The magnitudes of the preoperative main curves were severe, with a mean Cobb angle of 102.8 ± 16.9 degrees (range, 78 to 113 degrees). The mean flexibility of the main curve evaluated using supine side-bending films was 41 ± 16% (range, 25% to 72%). Kyphosis at the thoracolumbar area was recognized in all the patients, with a mean kyphosis angle of 49 ± 16 degrees (29 to 66 degrees). Dural ectasias were recognized in 3 patients. Surgical treatments using a growing rod system were performed in 2 patients (patients 1 and 2), and posterior correction and fusion surgeries were performed in 2 patients (patients 3 and 4) (Table 3). The mean correction rate of the main curve at the time of the initial surgery was 47 ± 15% (range, 44% to 51%). The thoracolumbar kyphosis corrections during the initial surgeries were satisfactory except in patient 3, who experienced a dislodgement of the cranial anchor during kyphosis correction. Cefazolin (20 to 40 mg/kg) was administrated intravenously as a prophylactic antibiotic in all the cases at 30 minutes before the start of the operation, 3 hours after incision, soon after the operation, and 12, 24, 36, or 48 hours after operation.

Regarding complications, intraoperative implant dislodgement occurred in 2 cases because of fractures of the facets and transverse process (patients 1 and 4). Postoperative implant dislodgement occurred in 2 patients (patients 2 and 4). One patient developed pseudoarthrosis at distal end of the fusion area (L3/4) with a correction loss of 14 degrees and a symptom of severe low back pain at 2 years after surgery (patient 3). She underwent revision surgery of posterior intervertebral fusion at L3/4 and L4/5. Deep wound infections occurred in 2 patients (patients 1 and 2), and eventually resulted in implant removal in 1 patient (patient 2). *Staphylococcus epidermidis* was isolated from patient 1, and Methicillin-susceptible *Staphylococcus aureus* was isolated from patient 2. Postoperative respiratory insufficiency requiring reintubation and ventilator

control for 3 days occurred in 1 patient (patient 4). Distal junctional kyphosis at L4/5 without any clinical symptoms was recognized in 1 case 4 years after the initial surgery (patient 4). An apparent increase in kyphosis from 10 degrees before surgery to 74 degrees at 6 years after surgery was recognized in the upper thoracic area (T1-T6) in 1 patient (patient 1).

Patient 1

A female patient was found to have scoliosis at the age of 6 months. Although she was followed by a pediatrician for an arterial septal defect, she was not referred to an orthopaedic surgeon until the age of 3 years, at which time her scoliosis had deteriorated to 80 degrees. She was referred to our department at the age of 3 years and 6 months; at presentation, she weighed 12.4 kg (− 1.4 SD) and was 103 cm tall (1.6 SD). X-ray films showed a triple major curve pattern with a Cobb angle of 53 degrees at T1-T7, 103 degrees at T7-L1, and 60 degrees at L1-5. The kyphosis angle at the thoracolumbar area (T9-L3) was 57 degrees. Surgical treatment using a growing rod system was begun at the age of 3 years and 7 months. Claw hooks were placed at T2 and T3 as proximal anchors, and pedicle screws were placed at L3 and L4 as distal anchors. Four months after the surgery, soon after the first rod lengthening, the bilateral proximal anchors were dislodged as a result of fractures of the transverse processes. Despite repeated proximal anchor replacements, the hooks dislodged 3 times and the pedicle screws dislodged once. Finally, the patient is treated by growing rod system with hooks at 3 levels of T1-3 as proximal anchors. However, the proximal thoracic kyphosis (T1-7) gradually increased to 74 degrees at 5 years after surgery. Thus, a brace treatment that regulated neck flexion was applied to prevent the progression of proximal thoracic kyphosis beginning 3 years after the first operation. The patient also suffered a deep wound infection at the proximal anchor site, which healed successfully after debridement and irrigation at 3 years and 6 months after surgery. *S. epidermidis* was isolated from the wound.

Patient 2

A male patient was observed by his mother to have a trunk deformity when he first stood up at the age of 10 months. However, he did not visit a pediatrician to receive treatment for his deteriorating trunk deformity until the age of 4 years and 1 month. He was diagnosed as having SGS and was referred to our department at the age of 4 years and 3 months for the treatment of his spinal deformity. His weight was 11.5 kg (− 1.1 SD) and his height was 98 cm (1.5 SD). He presented with the characteristic features of SGS, listed in Table 1 (Fig. 1). A missense mutation in the *FBN1* gene was identified using a polymerase chain reaction analysis. X-ray films showed a double major curve pattern with a Cobb angle of 79 degrees at T4-T11 and 100 degrees at T11-L4 (Fig. 2A). A kyphosis of 66 degrees was recognized at the thoracolumbar area (T11-L3) (Fig. 2B). Surgical treatment using a growing rod system was started at the age of 4 years and 10 months. During the first surgery, claw hooks were placed at T4 and

FIGURE 1. Clinical features of patient 2. The patient was a 4-year-old boy with a weight of 12.4 kg (− 1.1 SD) and a height of 103 cm (1.5 SD).

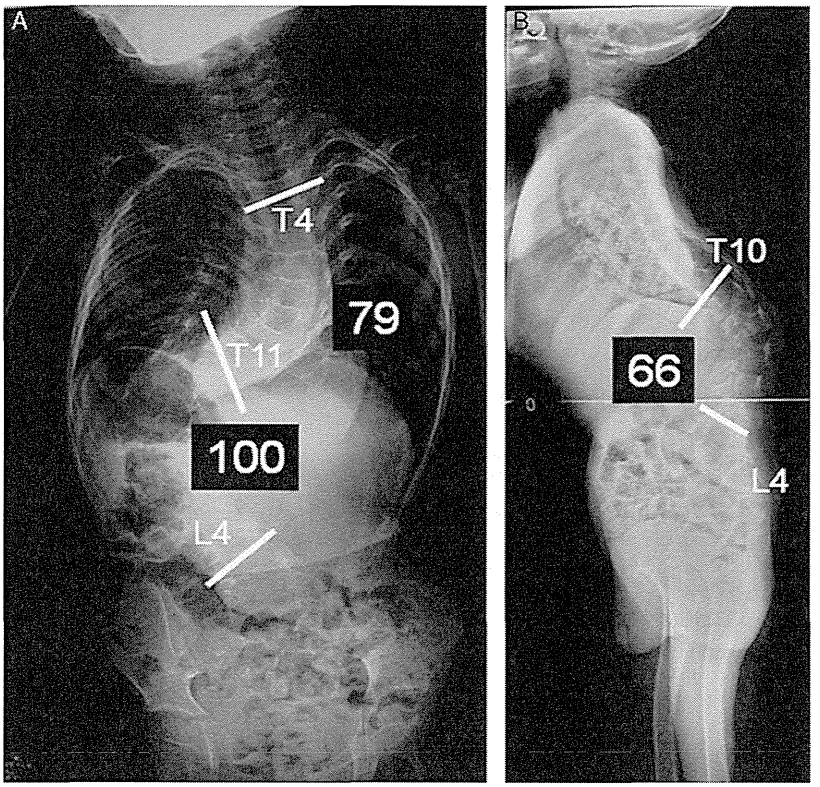

FIGURE 2. Preoperative radiographs of Patient 2. A double curve pattern with Cobb angles of 79 and 100 degrees (A) and local kyphosis of 66 degrees at the thoracolumbar junction are shown (B).

T5 as the proximal anchors and pedicle screws were placed only at L4 as distal anchors, as the patient was too thin to accommodate multiple screws. However, the hooks at T5 dislodged with fractures of the facets, possibly because of the poor bone quality, at the time of kyphosis correction using the cantilever technique. Postoperatively, the curves were corrected to 49 degrees at T4-T11 and 57 degrees at T11-L4, with correction rates of 38% and 45%, respectively (Fig. 3A). The kyphosis at the thoracolumbar area was corrected to 42 degrees (Fig. 3B). Five months after the surgery, the discharge of pus was recognized from a skin sore in the lumbar area just above the pedicle screws. As the infection did not subside after 2 surgical debridements, the distal anchors were removed at 9 months after the first surgery. Six months after their removal, growing rod treatment was restarted by placing distal anchors at L5. However, the deep wound infection recurred, and the implants were finally removed at 22 months after the first operation. At present, 6 years after the first surgery, the patient is being treated with a brace, and the Cobb angle of the main curve is 87 degrees (Fig. 3C) with a kyphosis of 125 degrees (Fig. 3D).

Patient 3

A female patient was found to have scoliosis at the age of 10 months. Although her scoliosis was pointed out by a plastic surgeon, her parents refused brace or surgical treatment for her. At the age of 11 years and 2 months, she was referred to our department for severe spinal deformity. She presented with the characteristic features of SGS, as listed in Table 1 (Fig. 4). X-ray films showed a double major curve pattern with a Cobb angle of 113 degrees at T5-T11 and 105 degrees at T11-L4 (Fig. 5A). A kyphosis of 44 degrees was recognized at the thoracolumbar area (T10-L3) (Fig. 5B). The Risser sign was 0, and the triradiate cartilages were closed. Posterior correction and fusion surgery were performed at the age of 11 years and 4 months. As her bone quality was poor, many segmental pedicle screws as possible were used to avoid implant dislodgement. Although an adequate number of pedicle screws were placed, the dislodgement of a few pedicle screws was observed on the concave side during curve correction. Moreover, a reduction in the motor-evoked potentials, which was restored after reversing the correction, was recognized during the curve correction. Thus, the endeavor to obtain a maximum correction was abandoned, and the main curves were corrected to Cobb angles of 50 and 52 degrees, respectively (Fig. 5C). The kyphosis at the thoracolumbar junction was corrected to 6 degrees (Fig. 5D). At 2 years after surgery, she developed pseudarthrosis at distal end of the fusion area (L3/4) with a correction loss of 14 degrees and a symptom of severe low back pain. She

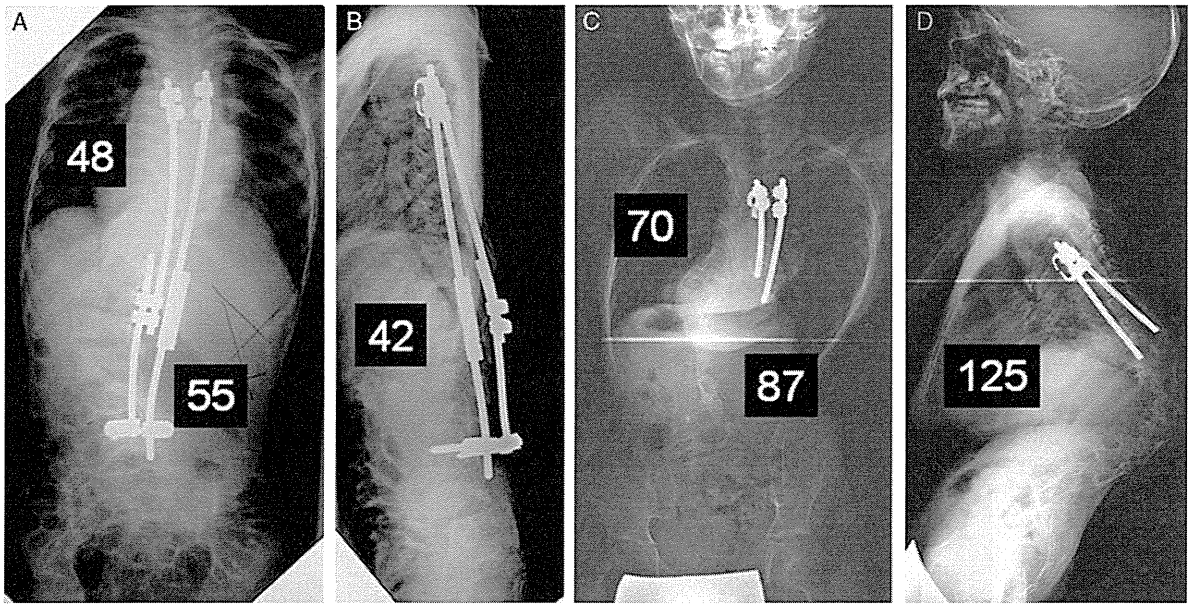

FIGURE 3. Postoperative radiographs of Patient 2. Growing rod treatment was started at the age of 4 years and 10 months (A, B). Postoperatively, the curves were corrected to 49 and 57 degrees (A). Kyphosis at the thoracolumbar area was corrected to 42 degrees (B). The distal anchors were finally removed due to deep wound infection at 22 months after the first operation. At present, 5 years after the first surgery, the Cobb angle of the main curve is 87 degrees (C) and the kyphosis is 125 degrees (D).

underwent revision surgery of posterior intervertebral fusion at L3/4 and L4/5. She was applied bed rest for 4 weeks and then trunk cast for 6 weeks after surgery.

Patient 4

A male patient was referred to our hospital at the age of 12 years and 6 months with a weight of 44 kg (0.1 SD) and a height of 164 cm (1.9 SD). Although he had been followed by a pediatrician for a cardiovascular problem and scoliosis was pointed out at the age of 7 years, he was not referred to an orthopaedic surgeon until the age of 12 years and 3 months; thus, no brace treatment was performed preoperatively. X-ray films showed a triple major curve pattern with a Cobb angle of 64 degrees at T1-T7, 78 degrees at T7-L1, and 52 degrees at L1-L5. A kyphosis of 29 degrees was recognized in the thoracolumbar area (T9-L3). The Risser sign was 0, and the triradiate cartilages were closed. Posterior correction and fusion surgery were performed at the age of 12 years and 9 months. As his bone quality was

FIGURE 4. Clinical features of Patient 3. The patient was a 10-year-old girl with a weight of 33 kg (−0.1 SD) and a height of 146 cm (1.6 SD).

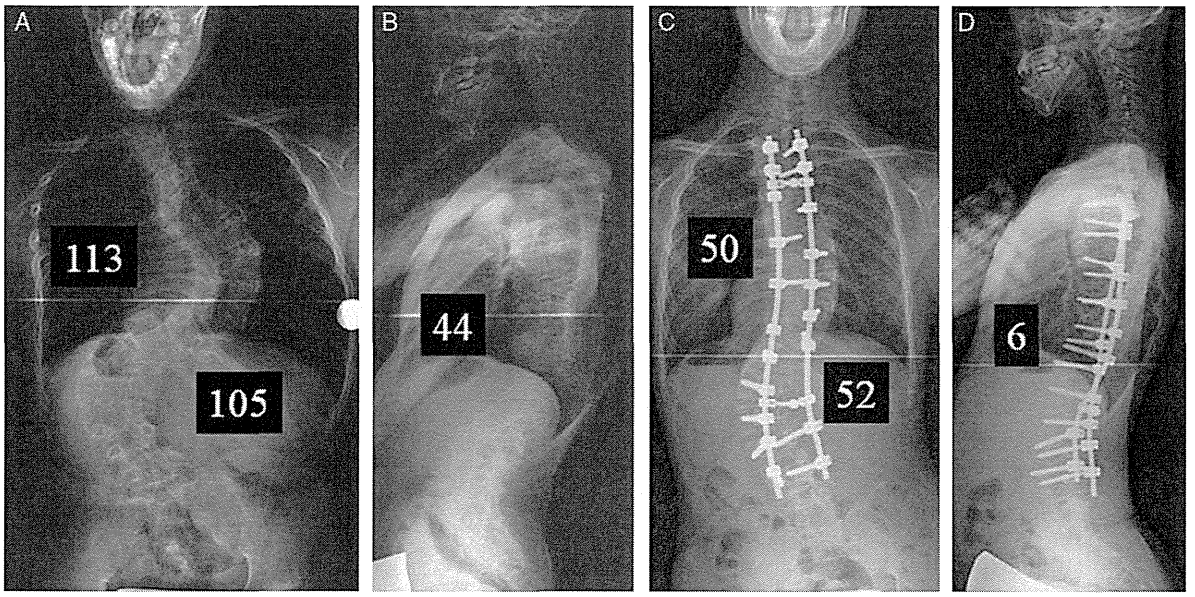

FIGURE 5. Radiographical findings of Patient 3. A double curve pattern with Cobb angles of 113 and 105 degrees (A) and local kyphosis of 44 degrees at the thoracolumbar junction are shown (B). Postoperatively, the main curves were corrected to Cobb angles of 50 and 52 degrees (C), and the kyphosis was corrected to 6 degrees (D).

poor, segmental anchors (screws, hooks) were placed at as many sites as possible to avoid implant dislodgement. However, the hooks at T1 were dislodged because of fractures of the transverse processes during curve correction. Ultrahigh molecular weight polyethylene fiber tapes (Alfresa Pharma, Osaka, Japan) were used to fix the rods to the T1 lamina, instead of using hooks. A reduction in motor-evoked potentials, which was restored after reversing the correction, was recognized during the curve correction. Postoperatively, the patient developed respiratory insufficiency requiring reintubation and assisted respiration for 3 days. Six months after the surgery, because of marked correction loss arising from the dislodgement of the proximal anchors, a revision surgery was performed and pedicle screws were placed at the right T1 and T2 and the left T2. Finally, the curves were corrected to 31degrees at T1-T7, 17 degrees at T7-L1, and 3 degrees at L1-L5. The thoracolumbar kyphosis was corrected to 42 degrees. The development of a junctional kyphosis of 13 degrees at L4/5, without any complaints, was recognized at 4 years after the first surgery.

DISCUSSIONS

The present series of patients with SGS indicated that the natural history of spinal deformity might start during infantile, and then finally would progress to very severe extent requiring surgical treatment. Unfortunately, none of the patients in this series had received brace treatment because the patients had been followed by doctors who might not have suspected the spinal deformities; thus, we could not know how effective brace treatment would be if brace treatment was applied within the extent of conservative treatment. However, as surgical treatment has a high risk of complications, we propose that thorough nonsurgical treatment including brace treatment or trunk cast be considered as alternative treatments to postpone surgical treatment as long as possible, especially in young kids as patient 1 or 2. If surgical treatments were not avoidable, preoperative evaluation by a pediatric cardiologist was compulsory as majority of the patient would accompany cardiac diseases. In addition, pulmonary function test including blood gas assessment should be performed suspecting restricted pulmonary dysfunctions or other malfunctions of respiratory system. The mean postoperative correction rate for the main curves (47%) was relatively low, compared with reported rates for severe scoliosis secondary to other diseases treated by pedicle screw construct.[12] One reason for this difference might be the poor bone quality, which prohibited large stresses on the anchors during correction. Another reason might be the rigidity of the curves in adolescents. The preoperative flexibilities were higher in the infants and much lower in the adolescents.

Intraoperative spinal cord monitoring of motor or sensory spinal evoked potentials should be performed during surgical treatment because the risk of injuring the spinal cord might be relatively high, as the correction of thoracolumbar kyphosis might increase the risk of neurological damage. In this study, reductions in motor-evoked potentials were recognized during curve corrections in 2 of the 4 cases. To prevent intraoperative neurological complications and/or to assess neurological

vulnerability preoperatively, halo gravity treatment[13] or extension over a bolster x-ray, may be a useful addition to the preoperative evaluations to determine the extent of the "safe" extension correction that can be achieved.

The surgical treatments for scoliosis in patients with SGS in our series were associated with a high complication rate. One such complication was implant dislodgement that was attributed to the extremely poor bone quality of the spine. In fact, hook or pedicle screw dislodgement was recognized during or after surgery in 3 of the 4 patients in this study. Such poor bone quality in patients with SGS might be related to an abnormality in fibrillin, which is considered to be associated with Marfan syndrome.[14,15] Kyphosis at the thoracolumbar area might also increase the risk of anchor dislodgement, as the correction of kyphosis places an excessive pull-out force on the anchors. Moreover, frequently observed dural ectasia associated with a narrowed pedicle and lamina can also increase the risk of anchor dislodgement. To prevent implant dislodgement, as many segmental anchors (screws, hooks, wires) as possible should be used. Hooks might be preferable to pedicle screws as proximal anchors when the pedicles are too narrow to accommodate pedicle screws. Additional sublaminar wiring or taping using ultrahigh molecular weight polyethylene fiber tapes should also be considered to reduce the risk of implant dislodgement. For growing rod treatment, anchor placements with abundant graft bone 3 to 4 months before curve correction with rod placement might be effective for patients with poor bone quality or severe kyphosis . Other techniques, such as preoperative halo gravity treatment,[13] anterior release, or intraoperative halo femoral traction,[16] which are often used for the surgical treatment of patients with severe deformities, should be considered. Postoperative brace application should also be considered to reduce the risk of implant dislodgement or pseudoarthrosis.

In our series, the 2 patients who were treated with growing rod systems developed deep wound infections after rod lengthening. The deep wound infections might have been associated with skin sores. All the 4 patients were skeletally very thin, with heights ranging from 1.5 to 1.9 SD for their ages and weights ranging from −1.4 to 0.1 SD. The prominence of implants caused by suboptimal implant coverage by the skin and subcutaneous tissues is a risk factor for wound infections, especially in patients treated with growing rod systems that require multiple surgeries. Thus, soft tissues should be handled with extreme care to prevent skin sores.

In conclusion, 4 patients with SGS who underwent surgical treatment for severe scoliosis are reported. Surgical treatment was associated with a high incidence of complications including implant failures and deep wound infections attributable to the poor bone quality and thin bodily habitus, which are characteristics of this syndrome.

REFERENCES

1. Shprintzen RJ, Goldberg RB. A recurrent pattern syndrome of craniosynostosis associated with arachnodactyly and abdominal hernias. *J Craniofac Genet Dev Biol*. 1982;2:65–74.
2. Ades LC, Morris LL, Power RG, et al. Distinct skeletal abnormalities in four girls with Shprintzen-Goldberg syndrome. *Am J Med Genet*. 1995;57:565–572.
3. Robinson PN, Neumann LM, Demuth S, et al. Shprintzen-Goldberg syndrome: fourteen new patients and a clinical analysis. *Am J Med Genet A*. 2005;135:251–262.
4. Greally MT, Carey JC, Milewicz DM, et al. Shprintzen-Goldberg syndrome: a clinical analysis. *Am J Med Genet*. 1998;76:202–212.
5. Saal HM, Bulas DI, Allen JF, et al. Patient with craniosynostosis and marfanoid phenotype (Shprintzen-Goldberg syndrome) and cloverleaf skull. *Am J Med Genet*. 1995;57:573–578.
6. Katzke S, Booms P, Tiecke F, et al. TGGE screening of the entire FBN1 coding sequence in 126 individuals with marfan syndrome and related fibrillinopathies. *Hum Mutat*. 2002;20:197–208.
7. Kosaki K, Takahashi D, Udaka T, et al. Molecular pathology of Shprintzen-Goldberg syndrome. *Am J Med Genet A*. 2006;140:104–108; author reply 109–110.
8. Hatchwell E. Shprintzen-Goldberg syndrome results from mutations in fibrillin-1, not monosomy 22q11. *J Pediatr*. 1997;131:164–165.
9. Sood S, Eldadah ZA, Krause WL, et al. Mutation in fibrillin-1 and the Marfanoid-craniosynostosis (Shprintzen-Goldberg) syndrome. *Nat Genet*. 1996;12:209–211.
10. Loeys BL, Chen J, Neptune ER, et al. A syndrome of altered cardiovascular, craniofacial, neurocognitive and skeletal development caused by mutations in TGFBR1 or TGFBR2. *Nat Genet*. 2005;37:275–281.
11. Watanabe Y, Yano S, Koga Y, et al. P1148A in fibrillin-1 is not a mutation leading to Shprintzen-Goldberg syndrome. *Hum Mutat*. 1997;10:326–327.
12. Watanabe K, Lenke LG, Bridwell KH, et al. Comparison of radiographic outcomes for the treatment of scoliotic curves greater than 100 degrees: wires versus hooks versus screws. *Spine*. 2008;33:1084–1092.
13. Rinella A, Lenke L, Whitaker C, et al. Perioperative halo-gravity traction in the treatment of severe scoliosis and kyphosis. *Spine*. 2005;30:475–482.
14. Carter N, Duncan E, Wordsworth P. Bone mineral density in adults with Marfan syndrome. *Rheumatology (Oxford)*. 2000;39:307–309.
15. Moura B, Tubach F, Sulpice M, et al. Bone mineral density in Marfan syndrome: a large case-control study. *Joint Bone Spine*. 2006;73:733–735.
16. Qiu Y, Liu Z, Zhu F, et al. Comparison of effectiveness of Halo-femoral traction after anterior spinal release in severe idiopathic and congenital scoliosis: a retrospective study. *J Orthop Surg*. 2007;2:23.

our data provide proof of concept support for targeting this molecule and its multi-cellular functions in psoriatic skin. Targeting VEGF topically may provide an effective new approach for treating mild-to-moderate psoriasis skin lesions by inhibiting angiogenesis and reducing leukocyte infiltration and KC proliferation.

Funding support

NLW is supported in part by grants from the National Institutes of Health (P30AR39750, P50AR05508, RO1AR063437; RO1AR062546) and the National Psoriasis Foundation.

Acknowledgments

The authors apologize to colleagues whose work could not be cited because of the space constraints. We thank Dr. John Rudge (Regeneron Pharmaceuticals, Tarrytown, NY) for providing VEGF-Trap and Dr. Thomas McCormick for feedback on the manuscript.

References

[1] Yancopoulos GD, Davis S, Gale NW, Rudge JS, Wiegand SJ, Holash J. Vascular-specific growth factors and blood vessel formation. Nature 2000;407:242–8.
[2] Kunstfeld R, Hirakawa S, Hong YK, Schacht V, Lange-Asschenfeldt B, Velasco P, et al. Induction of cutaneous delayed-type hypersensitivity reactions in VEGF-A transgenic mice results in chronic skin inflammation associated with persistent lymphatic hyperplasia. Blood 2004;104:1048–57.
[3] Jung K, Lee D, Lim HS, Lee S-I, Kim YJ, Lee GM, et al. Double anti-angiogenic and anti-inflammatory protein valpha targeting VEGF-A and TNF-alpha in retinopathy and psoriasis. J Biol Chem 2011;286:14410–18.
[4] Xia YP, Li B, Hylton D, Detmar M, Yancopoulos GD, Rudge JS. Transgenic delivery of VEGF to mouse skin leads to an inflammatory condition resembling human psoriasis. Blood 2003;102:161–8.
[5] Akman A, Yilmaz E, Mutlu H, Ozdogan M. Complete remission of psoriasis following bevacizumab therapy for colon cancer. Clin Exp Dermatol 2009;34:e202–4.
[6] Fournier C, Tisman G. Sorafenib-associated remission of psoriasis in hyperne-phroma: case report. Dermatol Online J 2010;16(17.).
[7] Wolfram JA, Diaconu D, Hatala DA, Rastegar J, Knutsen DA, Lowther A, et al. Keratinocyte but not endothelial cell specific overexpression of Tie2 leads to the development of psoriasis. Am J Pathol 2009;174:1443–58.
[8] Ward NL, Loyd CM, Wolfram JA, Diaconu D, Michaels CM, McCormick TS. Depletion of antigen-presenting cells by clodronate liposomes reverses the psoriatic skin phenotype in KC-Tie2 mice. Brit J Dermatol 2011;164: 750–8.
[9] Schonthaler HB, Huggenberger R, Wculek SK, Detmar M, Wagner EF. Systemic anti-VEGF treatment strongly reduces skin inflammation in a mouse model of psoriasis. Proc Natl Acad Sci USA 2009;21264–69.

Doina Diaconu[a], Yi Fritz[a], Sean M. Dawes[a], Candace M. Loyd[a], Nicole L. Ward[a, b, *]
[a]*Department of Dermatology, Case Western Reserve University, Cleveland, OH 44106, USA*;
[b]*The Murdough Family Center for Psoriasis, University Hospitals Case Medical Center, Cleveland, OH 44106, USA*

*Corresponding author at: Case Western Reserve University, Department of Dermatology BRB519, 10900 Euclid Avenue, Cleveland, OH 44106, USA.
Tel.: +1 216 368 1111; fax: +1 216 368 0212
E-mail address: Nicole.ward@case.edu (N. Ward)

19 April 2013

http://dx.doi.org/10.1016/j.jdermsci.2013.08.005

Letter to the Editor

Co-existence of mutations in the *FBN1* gene and the *ABCC6* gene in a patient with Marfan syndrome associated with pseudoxanthoma elasticum

To the Editor,

Marfan's syndrome (MFS) is a disease with an autosomal dominant mode of inheritance that is manifested by characteristic skeletal abnormalities, including arachnodactyly, cardiovascular lesions (such as aortic dilatation), and ocular manifestations (such as ectopia lentis) [1]. The *FBN1* gene [2], which encodes fibrillin-1 (a component of elastic fibers), has been identified as the responsible gene. Pseudoxanthoma elasticum (PXE) is an autosomal recessive disorder that causes the ectopic mineralization of elastic fibers in soft connective tissues and mainly affects the eyes, skin, and cardiovascular system. The precise pathomechanisms of elastic fiber degeneration in PXE have not been fully elucidated despite a number of extensive studies [3]. The disease is linked to mutations in the ATP-binding cassette sub-family C member 6 (*ABCC6*) gene [4,5]. Here, we report the case of a patient who exhibited the clinical manifestations of both MFS and PXE and in whom pathological gene mutations were detected in both the *FBN1* gene and the *ABCC6* gene.

In 2003, a 64-year-old, tall Japanese woman presented with skin eruptions in her nuchal area, axillae, and groin. She had previously experienced angina pectoris and had undergone bypass surgery for coronary stenosis. The patient's family history revealed that her mother had been tall and had died of heart disease when the patient was a small child. A history and physical examination of her father revealed that he had no noteworthy clinical findings. The patient was the 5th of 5 siblings, and the eldest sister and the 4th sister had both been tall. The eldest sister had suddenly died of unknown causes in early childhood, and the 4th sister had died of aortic dissection. The patient had two children, a 38-year-old son and a 36-year-old daughter, and both had skeletal abnormalities that included a tall stature and arachnodactyly. Her son had undergone a Bentall operation for aortic dissection and aortic valve regurgitation as a child. Dermatological and ophthalmological examinations revealed no evidence of PXE in either child. The patient's family tree is shown in Fig. 1A.

At the time of the patient's initial examination, she was 165 cm tall and had an arm span of 185 cm. Dolichocephaly, pectus carinatum, disproportionately long limbs for her height, and arachnodactyly were noted (Fig. 1B). Numerous papules ranging in color from normal to yellow arrayed in a cobblestone pattern were observed in the nuchal area, axillae, and groin (Fig. 1C). Ophthalmological examinations revealed angioid streaks on her retinas. Radiography revealed linear calcifications in the upper limbs. The pathological findings for skin biopsy specimens from the affected sites consisted of clumps of fragmented basophilic fibers in the middle and lower layers of the dermis (Fig. 1D). Granular deposits that stained positive with von Kossa stain (Fig. 1E) were observed in specimens from the same sites.

A genomic DNA analysis of the patient's blood revealed a monoallelic nonsense mutation (c. 5454C > A: exon 44, p.Cys1818Stop) in the *FBN1* gene (Fig. 2A). Exon sequencing of *ABCC6* was performed using primers designed to eliminate *ABCC6* pseudogenes for exons 1–9 [6] and those designed by Prime 3 for

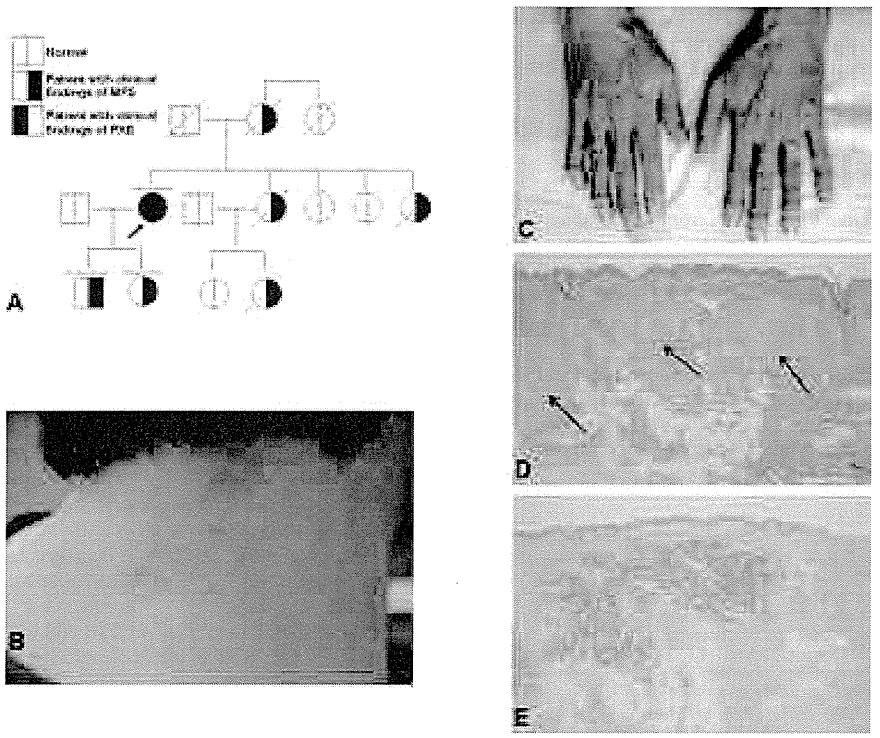

Fig. 1. Family tree, clinical findings, and pathological findings. (A) The patient's family tree. (B) Arachnodactyly. (C) Normal flesh color to yellow papules in a cobblestone pattern on the back of the patient's neck. (D) Clumps of fragmented basophilic fibers that look like thread waste are seen in the middle and lower layers of the dermis (hematoxylin and eosin, ×200). (E) Numerous granular deposits are seen among the clumps of fragmented fibers that have the appearance of thread waste (von Kossa stain, ×200).

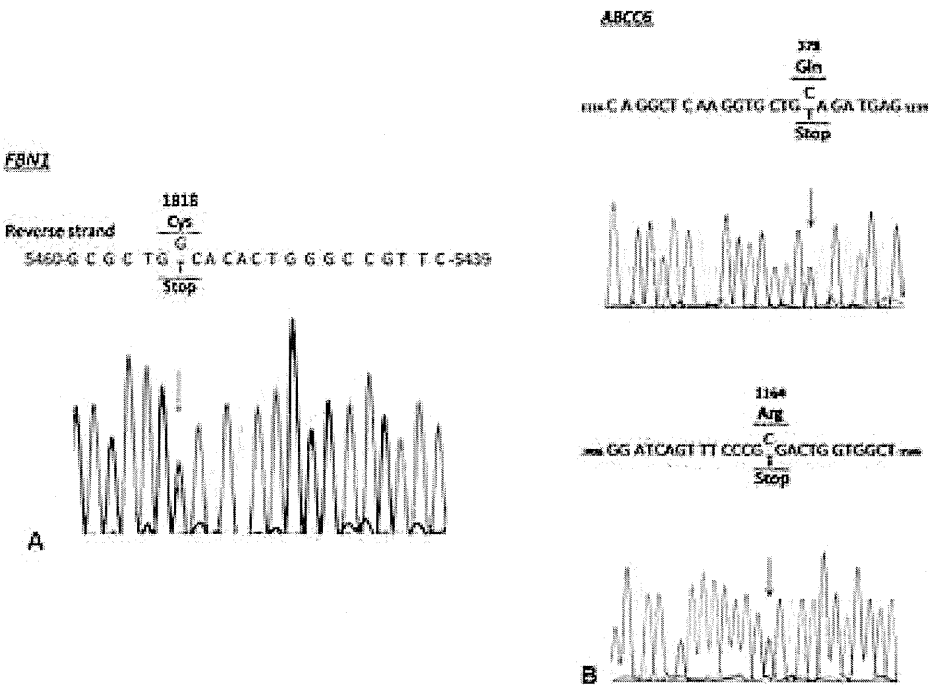

Fig. 2. Sequencing data of the patient's *FBN1* gene, which encodes fibrillin-1, and the *ABCC6* gene, which encodes ATP binding cassette C6 protein. (A) Sequence analysis of *FBN1*. A reverse sequence analysis of the portion of *FBN1* extending from c.5439 to c.5460 is shown. A monoallelic nonsense mutation (c.5454C > A, p.Cys1818Stop) was detected. (B) Sequence analysis of *ABCC6*. The results of sequence analyses of the portion of *ABCC6* extending from c.1116 to c.1139 and from 3486 to 3500 are shown. Compound heterozygous nonsense mutations (c.1132C > T, p.Gln378Stop and c.3490A > T, p.Arg1164Stop) were detected.

the other exons. The patient had two mutations in the ABCC6 gene: c.1132C > T in exon 9, p.Gln378Stop; and c.3490A > T in exon 24, p.Arg1164Stop (Fig. 2B). The patient's son had only the former mutation. Therefore, this patient had compound heterozygous nonsense mutations of *ABCC6*.

There has been one other report of a case of MFS and PXE in the same patient besides our own. The case was reported by Hidano et al. [7], similar to the present case, the previously reported patient was a member of a Japanese pedigree that exhibited the skeletal abnormalities associated with MFS, and the patient developed manifestations of both MFS and PXE. However, no search for gene mutations was performed in their case. Ours is the first report ever to describe MFS and PXE occurring in the same patient in whom mutations were confirmed in both the *ABCC6* gene and the *FBN1* gene. The concomitant presence of MFS and PXE seems to have been coincidental, but both conditions are hereditary diseases that give rise to elastic fiber abnormalities and to abnormalities in the same organs, including the cardiac blood vessels, and eyes. We plan to monitor the course of the presently reported patient to determine how her outcome compares with the outcome of patients who have only one of these diseases, either MFS or PXE.

References

[1] Burrows, Lovell CR. In: Tony B, Stephen B, Neil C, Christopher G, editors. Rook's textbook of dermatology. 7th ed., Oxford: Blackwell Science; 2004. p. 4621–31.
[2] Dietz HC, Cutting GR, Pyeritz RE, Maslen CL, Sakai LY, Corson GM, et al. Marfan syndrome caused by a recurrent de novo missense mutation in the fibrillin gene. Nature 1991;352:337–9.
[3] Uitto J, Li Q, Jiang Q. Pseudoxanthoma elasticum: molecular genetics and putative pathomechanisms. J Invest Dermatol 2010;130:661–70.
[4] Bergen AA, Plomp AS, Schuurman EJ, Terry S, Breuning M, Dauwerse H, et al. Mutation in *ABCC6* cause pseudoxanthoma elasticum. Nat Genet 2000;25:228–31.
[5] Lebwohl M, Nelder K, Pope FM, De Paepe A, Christiano AM, Boyd CD, et al. Classification of pseudoxanthoma elasticum. Report of a consensus conference. J Am Acad Dermatol 1994;30:103–7.
[6] Pulkkinen L, Nakano A, Ringpfeil F, Uitto J. Identification of ABCC6 pseudogenes on human chromosome 16p: implications for mutation detection in pseudoxanthoma elasticum. Hum Genet 2001;109:356–65.
[7] Hidano A, Nakajima S, Shimizu T, Kimata Z. Pseudoxanthoma elasticum associated with Marfan syndrome. Ann Dermatol Venereol 1979;106:503–5.

Shujiro Hayashi[a], Atsushi Utani[b], Akira Iwanaga[b], Yosuke Yagi[b], Hiroko Morisaki[c], Takayuki Morisaki[c], Yoichiro Hamasaki[a], Atsushi Hatamochi[a,*]

[a]*Department of Dermatology, Dokkyo Medical University, School of Medicine, Mibu, Tochigi, Japan*;
[b]*Department of Dermatology, Graduate School of Biomedical Sciences Nagasaki University, Nagasaki-city, Nagasaki, Japan*;
[c]*Department of Bioscience and Genetics, National Cerebral and Cardiovascular Center Research Institute, Suita, Osaka, Japan*
*Corresponding author at: Department of Dermatology, Dokkyo Medical University, School of Medicine 880 Kitakobayashi, Mibu, Tochigi 321-0293, Japan.
Tel.: +81 282 87 2154;
fax: +81 282 86 3470
E-mail address: hatamo@dokkyomed.ac.jp (S. Hayashi)

22 April 2013

http://dx.doi.org/10.1016/j.jdermsci.2013.07.007

Letter to the Editor

Birth, life, and death of the MAGE3 hypothesis of alopecia areata pathobiology

Dear Editor,

In this distinguished journal, we routinely read discovery stories that have been ultimately crowned by success. Instead, here we would like to share our trials and tribulations along a less felicitous, yet very instructive and educational research journey that brought us close to what we hoped to be a clinically important advance in understanding the pathobiology of alopecia areata (AA), a tissue-specific, T cell-dependent autoimmune disease [1].

Most currently available evidence suggests that, upon interferon (IFN)-γ-induced collapse of the hair follicle's (HF's) physiological immune privilege (IP), as yet unidentified follicular autoantigens are exposed to preexisting autoreactive $CD8^+$ T cells by ectopically expressed major histocompatibility (MHC) class I molecules within the epithelium of anagen hair bulbs [1,2]. Peptides derived from melanogenesis-associated autoantigens expressed only by melanin-producing anagen HFs are persuasive candidates as key autoantigens in AA [3]. Therefore, focusing on well-investigated MHC class I-restricted melanocyte-related antigens known to be recognized by $CD8^+$ T cells is a sensible AA research strategy (supplementary text S1).

Supplementary material related to this article can be found, in the online version, at http://dx.doi.org/10.1016/j.jdermsci.2013.07.014.

We thus hypothesized that it should be possible to detect cytotoxic $CD8^+$ T cells (CTLs) directed against MHC class-I restricted autoantigens (tyrosinase, MAGE-A2, and MAGE-A3 (MBL)), using pentamer technology [4] (Supplemental text S2). To test this hypothesis, peripheral blood mononuclear cells (PBMCs) were obtained from Japanese healthy controls and AA patients (Supplementary Table S1).

Initially, this approach yielded auspicious results: MAGE-A3-reactive $CD8^+$ T cells were found to be significantly increased in PBMCs in the acute phase of AA with multifocal lesions (AAM) and alopecia areata totalis (AAT) compared to healthy controls, chronic phase of AAM, or AAT/alopecia areata universalis (AU) (Fig. 1a and Fig. S1a and b and Supplementary text S3) ($p = 0.025$ by Kruskal–Wallis ANOVA). Furthermore, skin infiltrating T cells of an acute phase AA lesion from one patient, which were isolated as previously described [5], also showed an increased number of MAGE-A3 specific CTLs (Fig. 1b) as that in peripheral blood nuclear cells (PBMCs) from the same AA patients (Fig. 1c) compared to the average frequency of MAGE-$A3^+$ T cells in PBMCs from control subjects (Fig. 1a). This pilot finding suggested an enrichment of MAGE-$A3^+$ CTLs in lesional AA skin.

Supplementary material related to this article can be found, in the online version, at http://dx.doi.org/10.1016/j.jdermsci.2013.07.014.

Next, we probed whether such CTLs can produce IFN-γ after stimulation with MAGE-A3 (supplementary text S4). Indeed, IFN-γ protein expression was significantly increased in $CD8^+$ T cells from acute phase AA patients co-cultured with MAGE-A3 compared to healthy controls (Fig. 1d and supplementary Fig. S1c and d). Moreover, the percentage of MAGE-A3 specific CTLs